Rhythmic Growth-Induced Ring-Banded Spherulites with Radial Periodic Variation of Thicknesses Grown from Poly(ε-caprolactone) Solution with Constant Concentration

Zongbao Wang,[†] Giovanni C. Alfonso,[‡] Zhijun Hu,[§] Jidong Zhang,[†] and Tianbai He*,[†]

State Key Laboratory of Polymer Physics and Chemistry, Changchun Institute of Applied Chemistry, Graduate University of Chinese Academy of Sciences, Chinese Academy of Sciences, Changchun 130022, P. R. China; Department of Chemistry and Industrial Chemistry, University of Genova, Via Dodecaneso 31, 16146-Genova, Italy; and Laboratoire de Chimie et de Physique des Hauts Polymères (POLY), Université Catholique de Louvain, Place Croix du Sud 1, B-1348 Louvain-la-Neuve, Belgium

Received March 13, 2008; Revised Manuscript Received June 16, 2008

ABSTRACT: Birefringent ring-banded spherulites with radial periodic variation of thicknesses were grown from poly(ε-caprolactone) (PCL) solutions under conditions for which the solution concentration was held constant during the whole development of the morphology. The as-grown ring-banded spherulites were investigated by optical (OM) and atomic force (AFM) microscopies, by transmission electron microscopy (TEM) of samples sectioned parallel to the plane of film, and also by electron diffraction (ED) and grazing incidence X-ray diffraction (GIXD) techniques. The results indicate that the concentric rings in the birefringent ring-banded spherulites, as well as those in the nonbirefringent ring-banded spherulites, are a manifestation of periodic variation of thicknesses along the radius. The development of the ring-banded spherulites with radial periodic variation of thicknesses is due to periodic diffusion-induced rhythmic growth associated with periodical change in the concentration gradient in polymer solution with constant concentration. The morphological features reflect the competition between the diffusion flux of polymer chains in solution, J, and spherulitic growth with radial growth velocity, V, which can be characterized by the parameter $\delta = J/V$. The effects of crystallization conditions, including polymer molecular weight, initial solution concentration, and solvent evaporation rate, on the formation of ring-banded spherulites with radial periodic variation of thicknesses were studied.

Introduction

Formation of ordered structures and superstructures from disordered phases (solutions, melt, glassy state), is governed both by thermodynamics and kinetics. Because of their peculiar feature of being composed of flexible long chains, which make them very susceptible to local stimuli, polymers can be taken as model systems to gain an insight into the influence of kinetic factors on the development of crystal's structures and morphologies. It is important to understand what extent morphology and structure of polymer crystals is related to the kinetics of the succession of elementary processes underlying crystal growth which can be controlled through experimental variables such as temperature and concentration. The two competitive key processes determining the formation of crystalline morphology, especially for crystals grown in thin films,[1−6] are the diffusion of polymer chains toward the front of the developing crystal and the crystal's growth velocity. In the crystallization from the molten state, the two processes can be modulated, to some extent, only by changing the crystallization temperature. In melt crystallization, the two processes cannot be independently modulated; on increasing crystallization temperature, diffusion of polymer chains becomes faster while, at least up to relatively large undercooling, the crystal's growth velocity decreases.

On the other hand, at a given crystallization temperature, the diffusion of polymer chains and the crystal's growth velocity can easily be modulated when crystallization takes place in solution. This can be done by controlling the solvent evaporation rate and, consequently, the related concentration of the solution. In fact, different morphologies and structures can be obtained by controlling the solvent evaporation rate in polymer solution crystallization. In a previous study, we were able to affect the polymorphs of poly(di-*n*-butylsilane) crystals by controlling the solvent evaporation rate at around room temperature.[7] Both lozenge-shaped single crystals with 7/3 helical conformation and lath-shaped single crystals with all-trans conformation were obtained at relatively high solvent evaporation rate while only lath-shaped single crystals were originated when solvent was removed slowly. Even if it has been proved that structure and morphology of lamellar crystals can be modulated by controlling the solvent evaporation rate, the detailed understanding of the interplay among the various elementary processes leading to the final architecture of the crystalline aggregates remains a challenge.

In traditional solution crystallization, as growth of crystals proceeds, the concentration progressively decreases due to the consumption of chains as they feed the crystals. On the other hand, in conventional solution casting, in which solvent evaporation is not controlled, the crystal's growth velocity usually cannot keep up with the fast removal of solvent and the solution concentration progressively increases. Instead, the concentration can conveniently be modulated when the solvent evaporation rate is controlled during growth of crystals. In principle, the polymer concentration in the solution can be held constant if, at a given temperature, the increase of concentration due to solvent removal is exactly balanced by the depletion of concentration associated to the growth of the crystals.

In our previous work,[8] we have reported the formation of nonbirefringent ring-banded PCL spherulites, in which the chain axis is normal to the film plane, when crystallization is carried out under conditions of controlled slow solvent evaporation rate.

* To whom correspondence should be addressed. E-mail: tbhe@ciac.jl.cn. Fax: +86-431-85262126. Tel: +86-431-85262123.
[†] Graduate University of Chinese Academy of Sciences.
[‡] University of Genova.
[§] Université Catholique de Louvain.

10.1021/ma8005697 CCC: $40.75 © 2008 American Chemical Society
Published on Web 09/30/2008

These nonbirefringent ring-banded spherulites differ from the classical ring-banded spherulites in which lamellar crystals are periodically twisted along the radial growth direction.[9−17] Their concentric ring structure was attributed to structural discontinuities caused by rhythmic growth associated with periodic change in the concentration gradient, which is analogous to the material depletion reported by Duan et al.[18,19] and by Wang et al.[20] in polymer melt crystallization. According to the rhythmic growth mechanism,[8] the formation of nonbirefringent ring-banded spherulites is related to the amount of polymer chains per unit volume that diffuse to the crystallization front δ (mass/length^3), namely to the competition between diffusion flux of polymer chains in solution, J (mass/(time × length^2)), and spherulitic growth with the radial growth velocity, V (length/time).

In this paper, the development of PCL ring-banded spherulites with radial periodic variation of thicknesses is systemically studied and the rhythmic growth mechanism associated to periodic change in the concentration gradient is further discussed.

Experimental Part

Materials and Sample Preparation. Experiments were performed using a poly(ε-caprolactone) (PCL) sample with number-average molecular weight of 11 300 g/mol and polydispersity index (M_w/M_n) of 1.95 that was purchased from Polysciences Inc. The glass transition temperature (T_g) and melting point (T_m) of PCL were measured to be −60 and 60 °C, respectively. Solutions of PCL in toluene at the concentration of 5, 10, 20, and 50 mg/mL were prepared at room temperature. Ten μL of solution was cast at room temperature onto cleaned silicon wafers placed on a stage lodged inside a cylindrical container with radius and height 1.0 and 2.5 cm, respectively. The detailed preparation procedure was described in a previous paper.[8] Here, we recall that solvent evaporation rate was controlled by adding different volumes of extra toluene into the container, which was then covered with a lid. Under these conditions, solvent can only escape through the small gap between the container and its lid. The solvent evaporation rate was measured by weighing the container at different selected times. A slow solvent evaporation rate of 1.50×10^{-4} mL/h was achieved by adding 200 μL of extra solvent and keeping the container covered. It should be noted that the surface area of the solution keeps approximately constant during the process of solvent evaporation.

Calculation of Solution Concentration. To measure the concentration of the whole casting solution and the crystal's growth rate, samples were taken out from the container at different selected times during the evaporation process. Then the samples were held at room temperature for complete solvent evaporation until no further weight loss was detected. As it can be seen in Figure 1a, concentric ring-banded spherulites were observed when the solvent was slowly evaporated (1.50×10^{-4} mL/h); instead, small, nonbanded, spherulites develop around the already formed large ring-banded spherulites when the sample is exposed to air and the evaporation rate is much faster (6.92×10^{-2} mL/h).

Thanks to the clear difference in brightness between banded and nonbanded spherulites when observed by optical microscopy (OM) (Figure 1a), the total surface area of ring-banded spherulites was obtained by image analysis using Scion Image software. The ratio between the area of the ring-banded spherulites to that of the whole film, r_a, was used to calculate the corresponding concentration of polymer in the solution ϕ by the following equation:

$$\phi = \frac{m_p}{v_s}\frac{(1-r_m)}{(1-r_v)} \times 100\% = \phi_i \frac{(1-r_a c_d c_t)}{(1-r_v)} \times 100\%$$

where m_p, v_s, and ϕ_i are the polymer mass, the solvent volume, and the initial concentration of the cast solution deposited on the substrate, respectively. r_m is the ratio of the mass of ring-banded spherulites to the mass of whole polymer film m_p, and r_v is the ratio of the slowly evaporated volume of solvent within a given time to the initial solvent volume of the cast solution v_s. r_m can be calculated from r_a, by accounting for density and thickness differences between ring-banded and nonbanded birefringent spherulites (Figure 1a) through density and film thickness correction factors c_d and c_t, respectively. c_d is calculated from the crystallinity of the different types of spherulites, which can be measured by differential scanning calorimetry (DSC), and c_t is obtained from AFM results.

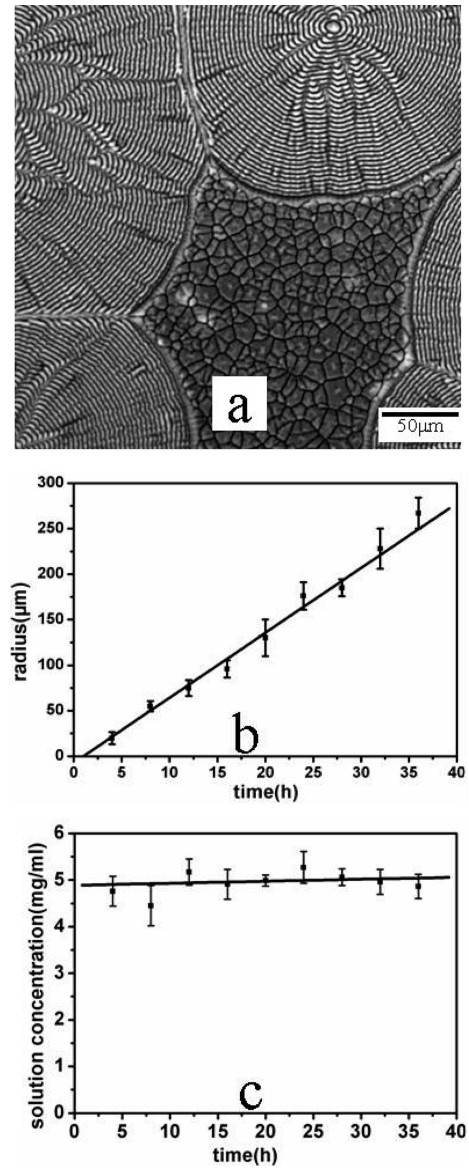

Figure 1. (a) Optical micrograph of PCL film taken out from the container during evaporation of the solvent from a 5 mg/mL toluene solution at 20 °C. The evaporation rate was 1.50×10^{-4} mL/h. (b) Radius of PCL ring-banded spherulites as a function of time. (c) Time dependence of the calculated concentration of the solution during evaporation of the solvent.

Since the radius of ring-banded spherulites increases with evaporation time, the growth velocity of concentric ring-banded spherulites was directly obtained by measuring their radius at different times during the controlled slow evaporation.

Instruments. Optical microscopy (OM) observations of the thin films were carried out using a Leica DMLP microscope equipped with a CCD camera.

The atomic force microscopy (AFM) experiments were performed with a SPA-300HV AFM equipped with a SPI 3800N controller (Seiko Instruments Industry Co., Ltd.). Pyramid-like Si_3N_4 tips, mounted on 100 μm triangle cantilevers with spring constants

of 0.09 N/m, were used. A 150 μm scanner was selected, and the contact mode was used to obtain height images.

Sections parallel to the film surface were observed by a JEOL JEM 1011 transmission electron microscope (TEM) with an accelerating voltage of 100 kV in bright field (BF) and electron diffraction (ED) modes. The polymer films deposited on the silicon wafer were first stained for 12 h in a saturated atmosphere of RuO_4 vapors to enhance the contrast between them and the epoxy matrix in which they were embedded to obtain ultrathin sections. Then, a layer of carbon was vacuum evaporated on the polymer surface before peeling off from the substrate by dipping into saturated KOH solution, floating in water, and collecting on a small piece of hardened epoxy. The epoxy pieces together with the polymer films were finally embedded in liquid epoxy and cured in three steps, lasting 12 h each, at progressively higher temperatures: 35, 45, and 55 °C. The ultrathin sections, ca. 70 nm thick, were microtomed at room temperature using a LEICA Ultracut R microtome and a glass knife. Slices were floated onto a water surface and retrieved with carbon-coated copper grids. Calibration of the electron diffraction spacing was carried out using Au.

Grazing incidence X-ray diffraction (GIXD) data were collected with a D8 Discover X-ray diffractometer (Bruker, Germany) (λ = 1.5406 Å) operated in the reflection mode.

Results and Discussion

Constant Concentration of the Polymer Solution during Growth of PCL Nonbirefringent Ring-Banded Spherulites. Nonbirefringent ring-banded spherulites were previously obtained at 20 °C from 5 mg/mL solution of PCL in toluene by controlling the solvent evaporation rate, R_{se}, at 1.50×10^{-4} mL/h.[8] To investigate the actual concentration of the solution during the development of this type of spherulites, OM observations on solution-cast films were carried out at nine selected evaporation times. From the series of micrographs collected at different times, which look pretty similar to the one shown in Figure 1a, the radius of nonbirefringent ring-banded spherulites was measured. Figure 1b demonstrates that the radius of the spherulites increases linearly with time over the whole duration of morphology development, as expected from interface kinetics models of Lauritzen and Hoffman.[21] Under above conditions, the radial growth velocity of the PCL spherulites, V, is 1.98 nm/s.

The concentrations of the polymer solution ϕ at different times during solvent evaporation were obtained by the equation shown in the Experimental Part. Therein c_d was calculated according to the relation: $c_d = \rho_{banded}/\rho_{nonbanded} = (\rho_c X_{c\ banded} + \rho_a(1 - X_{c\ banded}))/(\rho_c X_{c\ nonbanded} + \rho_a(1 - X_{c\ nonbanded}))$, where ρ_c is the density of 100% crystalline PCL and ρ_a is the density of amorphous PCL. The crystallinities of ring-banded and nonbanded spherulites were calculated according to the following relation: $X_c = (\Delta H_f/\Delta H^\circ_f \times 100\%$, where ΔH_f is the measured heat of fusion of the ring-banded or nonbanded spherulites and ΔH°_f is the heat of fusion of 100% crystalline PCL. According to the work published by Crescenzi et al.,[22] ΔH°_f of crystalline PCL is 135 J/g. ΔH_f of ring-banded and nonbanded spherulites are 118.26 and 79.33 J/g, respectively, from DSC results. So the $X_{c\ banded}$ and $X_{c\ nonbanded}$ were calculated to be 78.6% and 58.8%, respectively. On the basis of the density values reported in the literature (ρ_a = 1.081 g/mL[22] and ρ_c = 1.195 g/mL[23]), c_d was calculated to be 1.02. The other correction factor, c_t, can be calculated from AFM height results. The average film thickness of the nonbanded spherulites is 216 nm, as determined by AFM measurements after scratching with a blade. Examination of numerous height traces shows that the average thickness of banded spherulites is 3 nm smaller than the average film thickness of surrounding nonbanded spherulites zone. So c_t was calculated to be 0.986. As shown in Figure 1c, in which the average concentration calculated from several repeated experiments is plotted as a function of evaporation time, during the development of the nonbirefringent ring-banded spherulites the concentration of the solution keeps approximately constant at its initial value.

It is worth mentioning at this point that the volume of evaporated solvent is proportional to time while the mass of polymer chains which separates from the solution to form the ring-banded spherulites is proportional to square of time. Two possible reasons for the constancy of the concentration can be conceived. First of all, under the adopted conditions, the polymer solution has great self-adjusting capability, as will be discussed in detail in the following section. Second, ring-banded spherulites will inevitably impinge on one another as growth of spherulites proceeds. Some spherulites will encounter earlier because of the statistical nature of the formation of primary nuclei; this will produce nonuniform grain density and will cause a less than proportional relation between the amount of separated polymer chains and the square of time.

The growth rate of the spherulites, V, increases with decreasing crystallization temperature, T_c. As a consequence, if the solvent evaporation rate, R_{se}, is held constant, the solution tends to be more diluted at low than that at high T_c. Therefore, to obtain the regular ring-banded spherulites, R_{se} should be increased if T_c is lowered. As can be seen in Figure 2a−c, regular nonbirefringent ring-banded spherulites with similar band spacing could be obtained at 20, 10, and 0 °C, at which the growth rates are 1.98, 11.2, and 29.2 nm/s, by adjusting the evaporation rate, R_{se}, to 1.50×10^{-4}, 1.89×10^{-3}, and 4.75×10^{-3} mL/h, respectively. This is a further manifestation that constant concentration of the polymer solution is the basis for the formation of the regular nonbirefringent ring-banded spherulites.

Morphology and Structure of PCL Birefringent Ring-Banded Spherulites Obtained by Increasing δ. According to our previously reported results,[8] polymer chains in concentrated solution have larger flux J because of the occurrence of larger concentration gradient G. Since V is affected only slightly by the concentration of the solution (V increases from 1.98 to 3.00 nm/s when initial solution concentration is increased from 5 to 50 mg/mL), δ increases on increasing the concentration. At variance with dilute solutions, from which nonbirefringent ring-banded spherulites are obtained, birefringent ring-banded spherulites develop from concentrated solution. For example, in Figure 3 is shown a birefringent PCL banded spherulite grown in the same conditions as above (T_c = 20 °C and $R_{se} = 1.50 \times 10^{-4}$ mL/h), but from a solution 10 times more concentrated. Unlike classical PCL ring-banded spherulites that exhibit sharp contrast under crossed polarizers but very poor contrast under nonpolarized light,[24] as shown in Figure 3a and 3b, regularly spaced concentric ring structures are well evident in birefringent spherulites grown from concentrated solutions under both observation conditions. The birefringence in the thicker part of each band which appears under cross-polarized light possibly suggests that these spherulites, in addition to flat-on lamellae, also contain stacks of lamellar crystals with tilted orientation.

The morphology of these birefringent ring-banded spherulites was further investigated by AFM. The typical AFM topography image in Figure 4a clearly reveals the morphological details of the ring-banded structures. Alternation of ridges and valleys is well evident and this can be the reason for their optical properties. From Figure 4c it can be seen that the valleys correspond to locations in which lamellar crystals lie flat-on; the morphological evidence is confirmed by the corresponding ED pattern in which all evident diffraction spots can be assigned to (hk0) planes. Instead, as shown in Figure 4, d and e, tilted, and even edge-on, lamellae can be seen in proximity of the ridges. Some screw dislocations are evident in Figure 4d; this

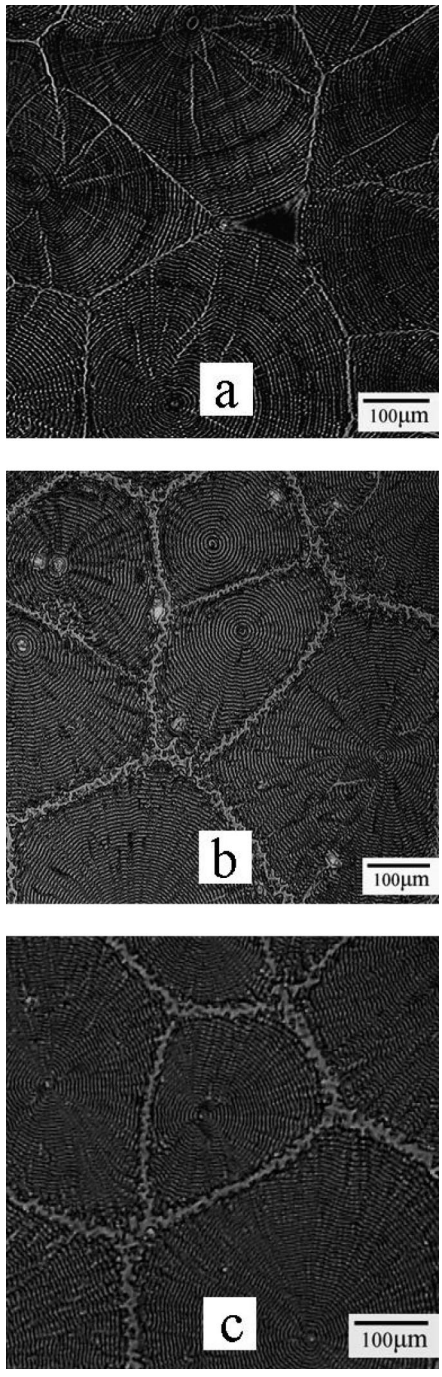

Figure 2. Optical micrographs in cross-polarized light of PCL films formed from 5 mg/mL toluene solution at different temperatures and solvent evaporation rates: (a) 20 °C, 1.50×10^{-4} mL/h; (b) 10 °C, 1.89×10^{-3} mL/h; (c) 0 °C, 4.75×10^{-3} mL/h.

suggests a similar initiation mode for new layers of lamellar crystals in nonbirefringent and birefringent ring-banded spherulites. It should be mentioned at this point that, both in valleys and ridges, PCL lamellae in align with their crystallographic *b*-axis oriented along the spherulitic radial growth direction.

The AFM results demonstrate that in both birefringent and nonbirefringent ring-banded spherulites the valleys consist of flat-on lamellar crystals, while at the surface of the ridges the orientation of the lamellae is different. It should be noted that the thickness of ridges in the birefringent banded spherulites (Figure 4b) is much larger than that in the nonbirefringent ones. To study whether the difference in thickness of ridges in nonbirefringent and birefringent banded spherulites is responsible for the variation of lamellar orientation, the internal

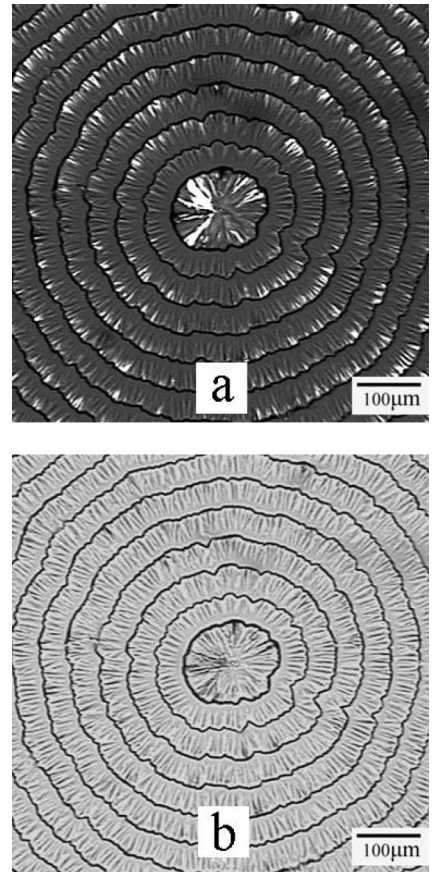

Figure 3. Optical micrographs of birefringent ring-banded PCL spherulites formed at the solvent evaporation rate of 1.50×10^{-4} mL/h from 50 mg/mL toluene solution at 20 °C: (a) cross-polarized light and (b) nonpolarized light.

morphology and structure of birefringent ring-banded spherulites were further investigated by TEM on ultrathin sections cut parallel to the plane of the film and GIXD experiments.

As shown in Figure 5, the morphology of lamellar crystals at different distance from the substrate can be discriminated in connected zones between PCL crystals films and epoxy films, confirmed by the corresponding ED patterns. The micrograph of Figure 5a shows that the first layer of ca. 400 nm next to the surface of the silicon wafer substrate is mostly formed by flat-on lamellae. Indeed, this is clearly demonstrated by the corresponding ED pattern which is composed of six diffraction spots that, on the basis of the orthorhombic unit cell of PCL crystals,[25,26] can be indexed as reflections from (200) and (110) planes. The morphological features and the corresponding ED patterns presented in Figure 5b−d suggest that the initially flat-on lamellae gradually twist and become more inclined as the distance from the substrate increases.

At intermediate distances, between ca. 400 and ca. 1000 nm, two additional reflections, which can be attributed to (012) planes, appear in the ED pattern. Since they are very close to the diffraction spots associated with (110) reflections, it is not always easy to get patterns in which they are clearly distinguishable. However, a close look at the full pattern obtained from slices cut at increasing distance from the substrate clearly indicates that while the intensity of the other spots decreases, the brightness of the (110 + 012) reflection intensifies. This is a manifestation, in the reciprocal space, of the tilting of the lamellae. When the distances from the wafer surface exceeds ca. 1600 nm, as shown in Figure 5e, the ED patterns collected in some areas only exhibits two strong (012) diffraction spots, thus indicating that far from the substrate the lamellae are preferentially oriented edge-on, as shown in Figure 5f.

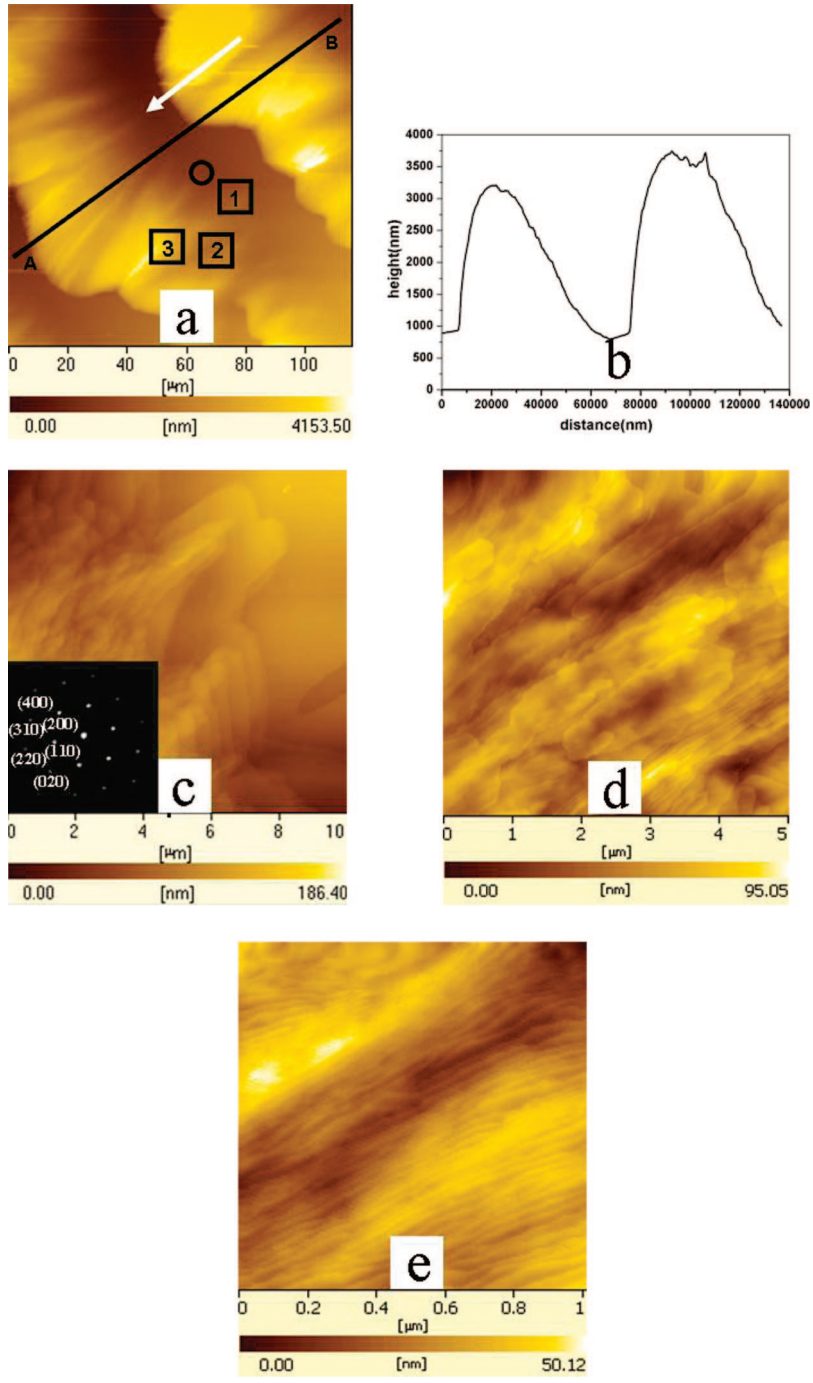

Figure 4. (a) AFM height image of PCL birefringent ring-banded spherulites formed at the solvent evaporation rate of 1.50×10^{-4} mL/h from 50 mg/mL toluene solution at 20 °C. The radial growth direction is indicated by the arrow. (b) Height profile corresponding to the line between points A and B in (a). (c) High-resolution AFM height image of the dark band in the position indicated by the square 1 and ED pattern obtained in correspondence of the circle in (a). (d and e) High-resolution AFM height image of the bright band in the regions shown by the squares 2 and 3, respectively.

To confirm the consistency between morphological features and ED patterns in ultrathin sections, flat-on lamellar crystals were tilted around the crystallographic *b*-axis to obtain ED patterns with different tilt angle. With no tilt, the ED pattern contains two (200) spots and four (110) spots; when the tilt angle is ca. 36°, some evidence of appearance of the (012) diffraction spots is obtained. Two strong (012) reflections feature the ED pattern of flat-on lamellae tilted to 45°. Altogether, the observed morphologies and the associated ED patterns prove that the lamellae in the birefringent ring-banded spherulites gradually tilt and take different orientation with increasing the distance from the substrate.

Figure 6a shows GIXD pattern of the birefringent ring-banded spherulites collected at different incidence angles of 0.15°, 0.20°, 2.00°, and 5.00°, respectively. The four peaks at $2\theta = 10.3°$, 13.0°, 15.7°, and 23.8° can be assigned to the reflections from (002), (101), (102), and (200) crystalline planes of PCL, respectively.[25,26] The patterns also contain a broad peak, at about $2\theta = 21.0°$, which cannot easily be assigned. However, two very close reflections corresponding to (012) and (110) planes are expected in this angular range; the first one at 20.6° and the second at 21.4°.[25,26] Therefore, in agreement with the ED evidence discussed above, the broad peak can be considered as

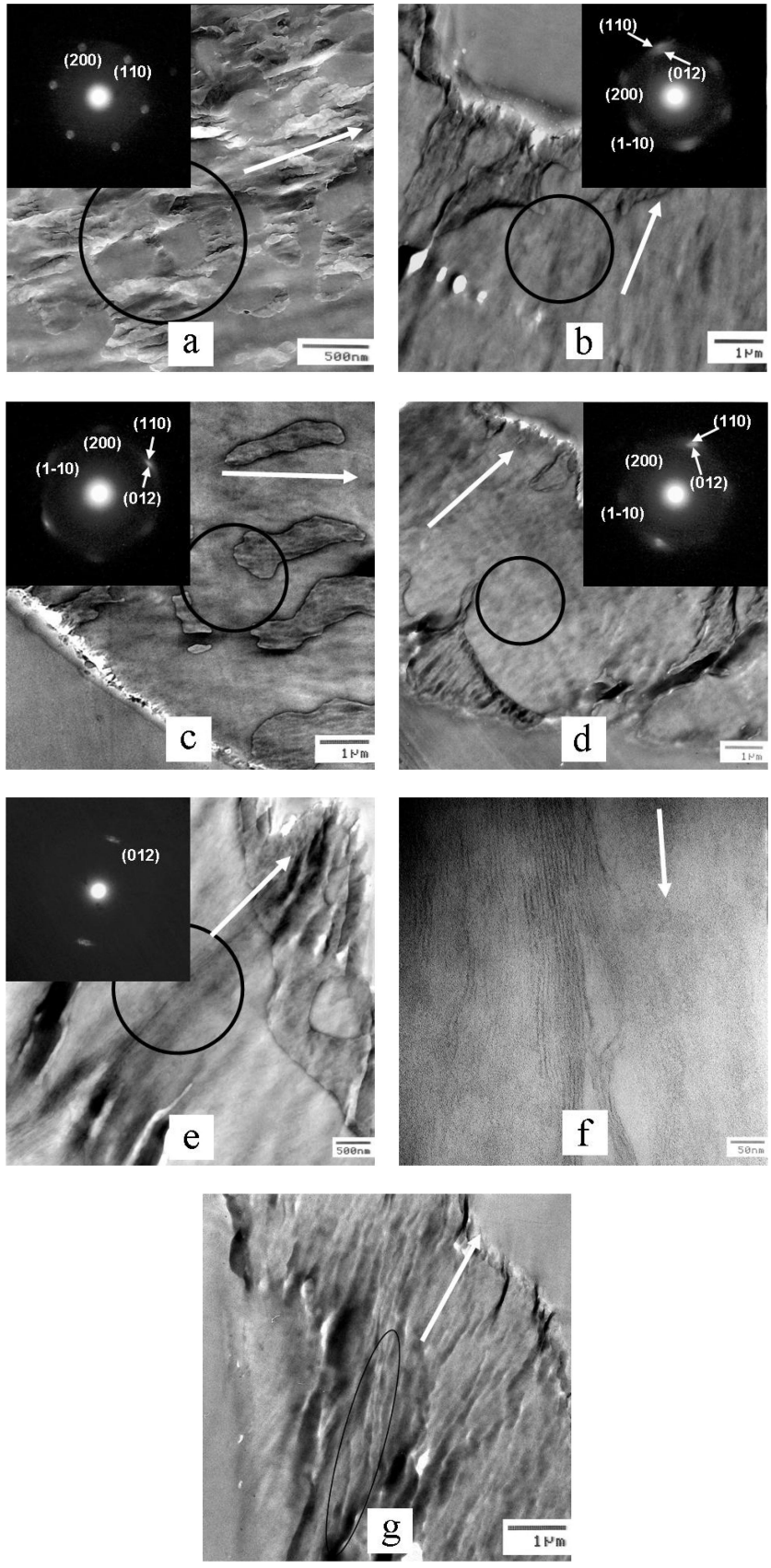

Figure 5. BF images of ultrathin sections, cut at different heights from the substrate, of birefringent ring-banded spherulites and ED pattern corresponding to the area indicated by the circle. Distance from the substrate: (a) ca. 0 to <400 nm; (b) ca. 400 to <600 nm; (c) ca. 600 to <1000 nm; (d) ca. 1000−1600 nm; (e, f, g) above ca. 1600 nm. The radial growth direction is indicated by the white arrow.

being originated by the contribution of (012) and (110) reflections.

The intensity of the (102) and (002) reflections, normalized to that of the (200) peak, is plotted as a function of the incidence

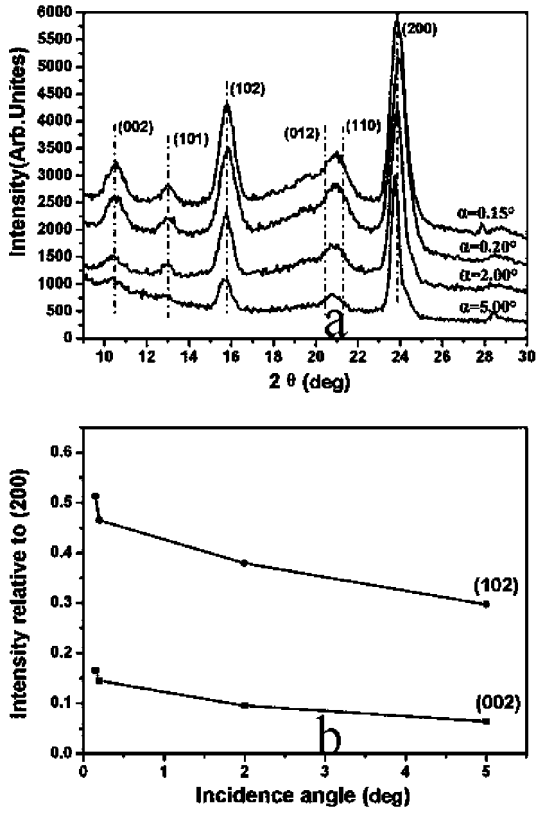

Figure 6. (a) GIXD pattern of PCL birefringent ring-banded spherulites collected at different incidence angles. (b) Intensities of (102) and (002) diffraction peaks, normalized to that of the (200) plane, as a function of the incidence angle.

angle in Figure 6b. The observed decrease of both $I_{(102)}/I_{(200)}$ and $I_{(002)}/I_{(200)}$ on increasing the incidence angle is a direct consequence of the changing penetration depth of the X-ray beam. The greater the angle, the thicker the volume from which signals are originated. In agreement with the TEM and ED results discussed above, (200) reflections are indicative of flat-on lamellae while (102) and (002) diffraction peak are associated with inclined and edge-on orientation; therefore, also GIXD results demonstrate that the orientation of lamellae gradually changes from being flat, close to the substrate surface, to be largely inclined and even edge-on in the top layers of ridge bands. Summarizing, the bottom layers and the valleys of birefringent PCL spherulites are mainly composed of lamellae lying on the plane of the substrate; in the intermediate layers, between ca. 400 and 1600 nm, stacks of inclined lamellar crystals coexist together with flat-on lamellae; finally, lamellae with any orientation, including edge-on, can be found in the top layer of ridge bands above ca. 1600 nm. As shown in Figure 5g, twisted lamellae can be found in the top layers of the ridges, but no evidence of continuous radial periodic twisting, as in the classical melt crystallized ring-banded spherulites, has been found. Therefore, in the PCL birefringent ring-banded spherulites obtained from relatively concentrated solutions, the lamellae rotate out of the film plane as the distance normal to the substrate increases.

According to the morphological and structural results discussed above, in birefringent ring-banded spherulites the planar orientation of lamellar crystals, which characterizes the nonbirefringent ring-banded spherulites, is lost on increasing thickness. The concentric rings of both birefringent and nonbirefringent ring-banded spherulites are only due to the radial periodic variation of their thicknesses.

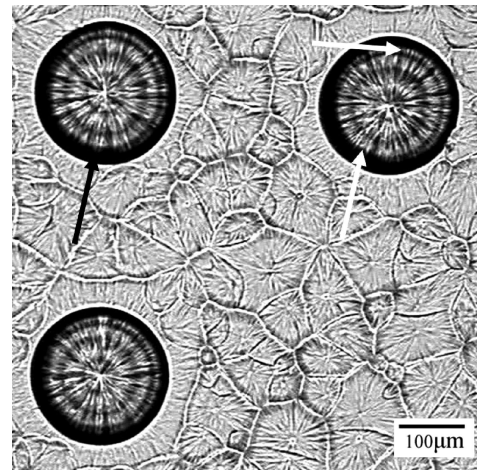

Figure 7. OM images in nonpolarized light of PCL birefringent banded and nonbanded spherulites. The film was removed from the container during evaporation of the solvent at 20 °C and at a rate of 1.50×10^{-4} mL/h from 50 mg/mL toluene solution.

Rhythmic Growth Mechanism of PCL Ring-Banded Spherulites with Radial Periodic Variation of Thicknesses. The ring-banded spherulites exhibiting radial periodic variation of thickness are clearly different from the classical ones in which lamellar crystals are periodically twisted along their radial growth direction. In analogy to the development of Liesegang rings in small molecule solution systems, their formation can be described by a periodic diffusion-induced rhythmic growth associated with periodic changes in the concentration gradient.[27] The growth of ringed-banded spherulites with radial periodic variation of thickness reflects the competition between the diffusion flux of polymer chains in solution, J (mass/(time $\times$ length^2)), and spherulitic growth with radial velocity, V (length/time), which dictates the amount of polymer chains per unit volume that diffuse to the crystallization front $\delta = J/V$ (mass/length^3).

As has been previously discussed, the concentration of the whole solution keeps approximately constant during the development of spherulites. However, at the front of the growing spherulites there is a layer in which the concentration is depleted because the diffusion-driven incoming polymer chains are insufficient to replace those consumed by the growth process. By all means this situation is similar to that found in thin films crystallization from the melt.[19] As evidenced by the dark ring indicated with the black arrow in Figure 7, there is a depletion region around the ring-banded spherulites in which almost no polymer seems to be present. We denote with l the thickness of this region along the growth direction which, as schematically shown in Figure 8, corresponds to the diffusion length of polymer chains in the solution. Accordingly, the radial concentration gradient, G (mass/length^4), can be written as: $G = (\phi_\infty - \phi_0)/l$, where ϕ_0 is the polymer concentration in the solution adjacent to the growth front, which is close to zero, and ϕ_∞ is the concentration at radial distances larger than l, which actually corresponds to the whole solution concentration. Thus, according to Fick's first diffusion law, the diffusion flux of polymer chains, J (mass/(time $\times$ length^2)), from the bulk of the solution to the growth front of the spherulites is given by the product of the diffusion coefficient, D (length^2/time), and the radial concentration gradient: $J = DG = D(\phi_\infty - \phi_0)/l$ and the amount of polymer chains per unit volume that diffuses to the crystallization front, δ (mass/length^3), is given by $\delta = D(\phi_\infty - \phi_0)/lV$.

On these bases, the development from solutions of ring-banded PCL spherulites with radial periodic variation of thickness can be explained by using the sequence of schematic

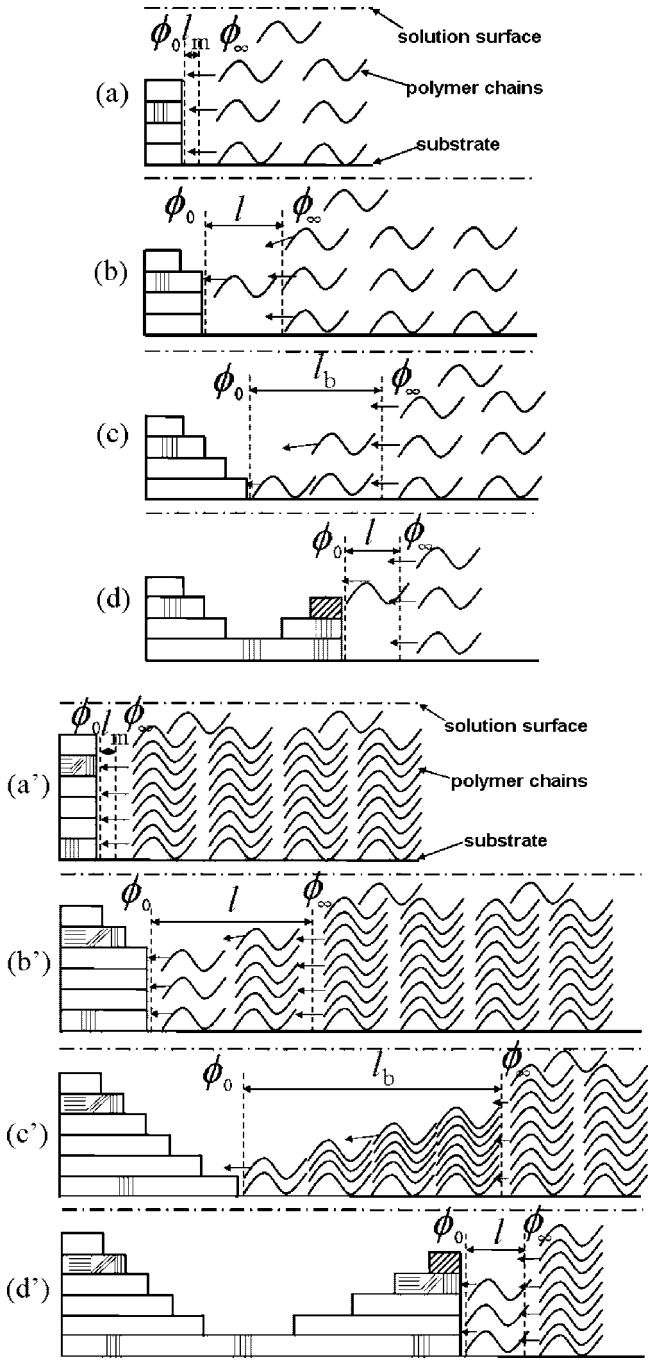

Figure 8. Model for the development of PCL ring-banded spherulites with radial periodic variation of thickness. The orientation of chains in the lamellae is indicated by parallel lines. (a−d) dilute solution, (a′−d′) concentrated solution. (a,a′) at the ridges of the bands: diffusion length has the minimum value, l_m, and concentration gradient G is the largest. (b,b′) diffusion length gradually increases while the concentration gradient decreases; crystals in the top layer cannot grow and thickness of the spherulite sharply decreases. (c,c′) in correspondence of the valleys of the bands: diffusion length increases to its limiting value, l_b, while the concentration gradient further decreases; in most of the layers growth has stopped. (d,d′) from valleys to ridges: lamellar crystals grow upward and forward; gradual decrease of diffusion length and increase of concentration gradient G; screw dislocations initiate new layers (hatched).

diagrams shown in Figure 8. In correspondence with the ridges, G is the largest and the diffusion length l is at its minimum value, l_m (Figure 8a,a′). As the lamellar crystals grow forward, the concentration of polymer chains in the layer adjacent to the growth front quickly decreases. This implies that, to feed the crystal, polymer chains from neighboring regions, thus traveling over longer distances, are needed. The increase of the diffusion length reduces the radial concentration gradient and the condition for which, at the growth front, the amount of polymer is no longer sufficient to supply material for the growth of the crystals in the top layers of the spherulites can be attained. Under this circumstance, the lamellae in the ridges cannot grow any longer and the thickness of the spherulite sharply decreases (Figure 8b,b′). As long as diffusion provides to the growth front fewer chains than those required for the continuous growth with constant thickness, the developing spherulite tends to become thinner. However, with the reduction of thickness, less feed is required to enable the spherulite to spread radially. The reduced consumption of polymer chains by the thin growth front allows diffusion to refill the solution and to gradually restore the initial concentration gradient. Coupled with the accompanying decrease of the required diffusion distance, this promotes the upward development of new layers on the top of the existing ones, likely initiated by screw dislocations, and their growth in the radial direction. Accordingly, the periodic variation of the concentration gradient is responsible for the rhythmic variation in the thickness of the banded spherulites grown from solutions. When G is at its minimum value, growth of most lamellar crystal layers has stopped and the instantaneous growth front with minimum thickness corresponds to a valley in the banded spherulite (Figure 8c,c′). On the other hand, with the gradual increase of G and decrease of l, the thickness of the ring-banded spherulite increases until, in correspondence to the ridge, the polymer chains at the growth front are consumed too fast to be replaced by those diffusing from the bulk of the solution. (Figure 8d,d′). The ring-banded spherulites with radial periodic variation of thickness are produced through a repetition of the rhythmic growth process schematized in Figure 8. According to the spherulitic growth process described above, l should be periodically self-adjusting between l_b and l_m because of the periodic imbalance of supply and demand of polymer chains at the growth front. Therein l_b is comparable with half of the band spacing and l_m is close to zero. Therefore, on the average, the diffusion length in PCL solution is ca. 100 times longer than that previously found in the melt crystallization of isotactic polystyrene thin films.[19]

It should be mentioned at this point that there is no periodic fluctuation of the whole solution concentration during the development of birefringent banded spherulites. As they grow, the consumption of polymer chains in the ridges is greater than that in the valleys because of the different number of lamellae that must be simultaneously fed. If all ring-banded spherulites grew synchronously, the whole solution concentration should periodically fluctuate; this is not the case because the bands do not grow synchronously, even in the same spherulite. As indicated by white arrows in Figure 7, the instantaneous growth front can simultaneously be in correspondence with a valley or of a ridge.

Effect of Changing δ on the Formation of the Ring-Banded Spherulites with Radial Periodic Variation of Thickness. According to the described growth mechanism, the amount of polymer chains per unit volume that diffuse to the crystallization front, δ, affects the development of periodic radial variation of thickness in ring-banded PCL spherulites. Since $\delta = D(\phi_\infty - \phi_0)/lV$, it is directly proportional to D and ϕ_∞, and inversely proportional to the spherulitic growth rate, V. To verify whether the suggested rhythmic growth mechanism is adequate to explain experimental evidence and to better understand how the periodic radial variation of thickness originated, we studied the effect of variables such as polymer molecular weight, M_n, initial solution concentration, ϕ_i, and solvent evaporation rate, R_{se}, which are expected to have an influence on D, ϕ_∞, and V, on the formation of ring-banded spherulites.

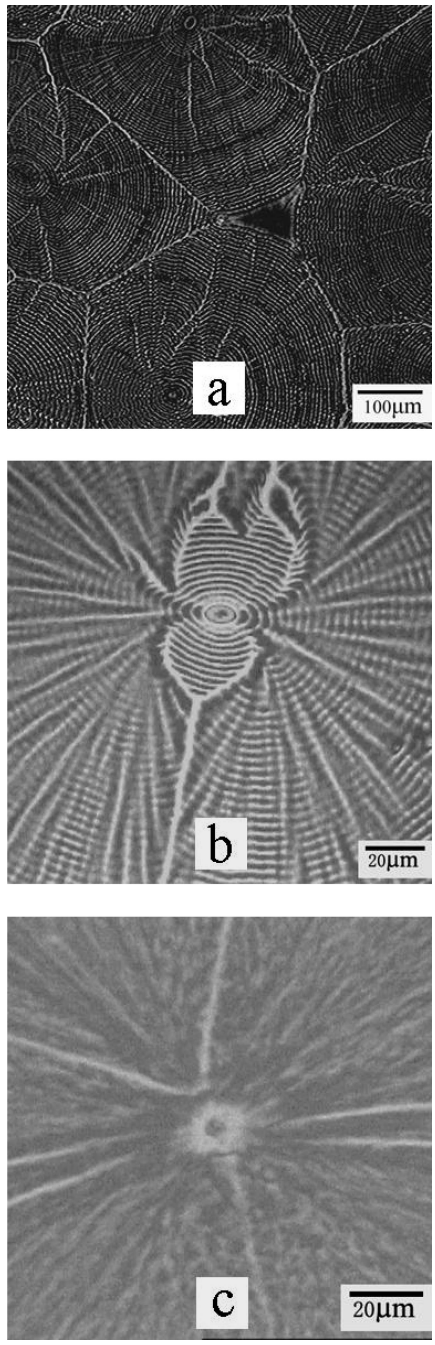

Figure 9. OM images in cross-polarized light of nonbirefringent ring-banded PCL spherulites grown at 20 °C from 5 mg/mL toluene solutions. The same low evaporation rate of 1.50×10^{-4} mL/h was imposed. The molecular weights of the PCL samples were (a) 11 300, (b) 20 200, and (c) 84 400.

In Figure 9, the series of OM images of PCL spherulites, grown at 20 °C in a 5 mg/mL toluene solution from which the solvent was evaporated at a rate of 1.50×10^{-4} mL/h, illustrate the effect of M_n on the banding periodicity. On increasing the polymer molecular weight from 11 300 to 20 200, the band spacing decreases from 5.46 to 3.03 μm while no banding is seen with the highest M_n sample. This experimental evidence is well in line with the expectations. In fact, thanks to the independence of the free energy of the folding surface from M_n for PCL with high molecular weight ($M_n > 10\,000$),[28] the growth rate of the lamellae should be roughly the same for the different polymers; on the other hand, the diffusion coefficient certainly decreases on increasing molecular dimensions. Accordingly, the greater the molecular weight, the smaller is δ, resulting in smaller band spacing.

It should be mentioned at this point that no bands form with the highest molecular weight sample and that their ED patterns indicate that the spherulites obtained in the above experimental conditions are mostly constituted of flat-on lamellae. However, if V is increased to 242 nm/s by changing crystallization conditions, δ decreases drastically, resulting in the formation of classical ring-banded spherulites with periodic twisting of lamellar crystals along the radial growth direction of the spherulites.[29]

In the series of optical micrographs of Figure 10, the ring-banded spherulites formed at the R_{se} of 1.50×10^{-4} mL/h from toluene solution with different concentration at 20 °C are shown. Nonbirefringent ring-banded spherulites develop from 5 and 10 mg/mL solutions, while birefringent ring-banded spherulites form in 20 and 50 mg/mL solutions. It is worth recalling that, on the basis of several measurements and using the equation reported in the Experimental Part, at least for the 10, 20, and 50 mg/mL solutions the concentration keeps approximately constant at its initial value during the development of spherulites. The growth rate of the spherulites developing from solutions at different concentration has been measured and it has been ascertained that it is only slightly affected by this variable: on increasing the concentration by 1 order of magnitude, from 5 to 50 mg/mL, an increase of 50% was measured in the growth rate, from 1.98 to 3.00 nm/s. In line with the proposed model, an increase of band spacing is expected on increasing the concentration of the solution. Indeed, we have measured band spacing of 5.46 ± 0.46, 13.2 ± 2.4, 26.3 ± 3.8, and 48.2 ± 4.2 μm for the solutions with concentration of 5, 10, 20, and 50 mg/mL, respectively. Because the more concentrated solution has greater self-adjusting capability for what concerns local concentration fluctuation, more regular ring-banded structures are obtained.

Figure 11a−d shows a series of OM images illustrating the effect of R_{se} on the formation of PCL ring-banded spherulites. Band spacings of 5.46 ± 0.46, 28.3 ± 9.7, and 42.6 ± 9.5 μm were measured in the spherulites formed at solvent evaporation rates, R_{se}, of 1.50×10^{-4}, 1.03×10^{-3}, and 2.80×10^{-3} mL/h, respectively. Instead, no bands were detected in the small spherulites obtained by evaporating the solvent at a rate of 6.92×10^{-2} mL/h. On increasing R_{se}, the ridge bands gradually tend to become wider while the width of the valleys does not change. At the lowest evaporation rate ($R_{se} = 1.50 \times 10^{-4}$ mL/h) the concentration of the polymer solution keeps approximately constant during the development of the nonbirefringent banded spherulites which growth at a linear rate of 1.98 nm/s. Instead, under fast evaporation conditions ($R_{se} = 6.92 \times 10^{-2}$ mL/h), the concentration of the solution progressively increases until saturation occurs because the velocity at which chains are captured by the developing crystals cannot successfully compensate the loss of solvent. As shown in Figure 11d, nonbanded spherulites which grow with radial velocity of 26.85 nm/s are formed in these conditions. When R_{se} is between 1.50×10^{-4} and 6.92×10^{-2} mL/h, the concentration of the solution increases until a balance between the effects of spherulitic growth and solvent evaporation rate establishes close to the growth front. Therefore, an increase of R_{se} leads to an increase of the concentration which, in turn, produces larger band spacing. With $R_{se} = 1.03 \times 10^{-3}$ mL/h, the concentration of the solution gradually increases and this is reflected by the parallel increase of the banding periodicity along the radius of the nonbirefringent ring-banded spherulites which grow at a rate of 4.36 nm/s (Figure 11b). If R_{se} is further increased to 2.80×10^{-3} mL/h, birefringent ring-banded spherulites growing at $V = 9.65$ nm/s are formed. (Figure 11c). Fluctuations in the band

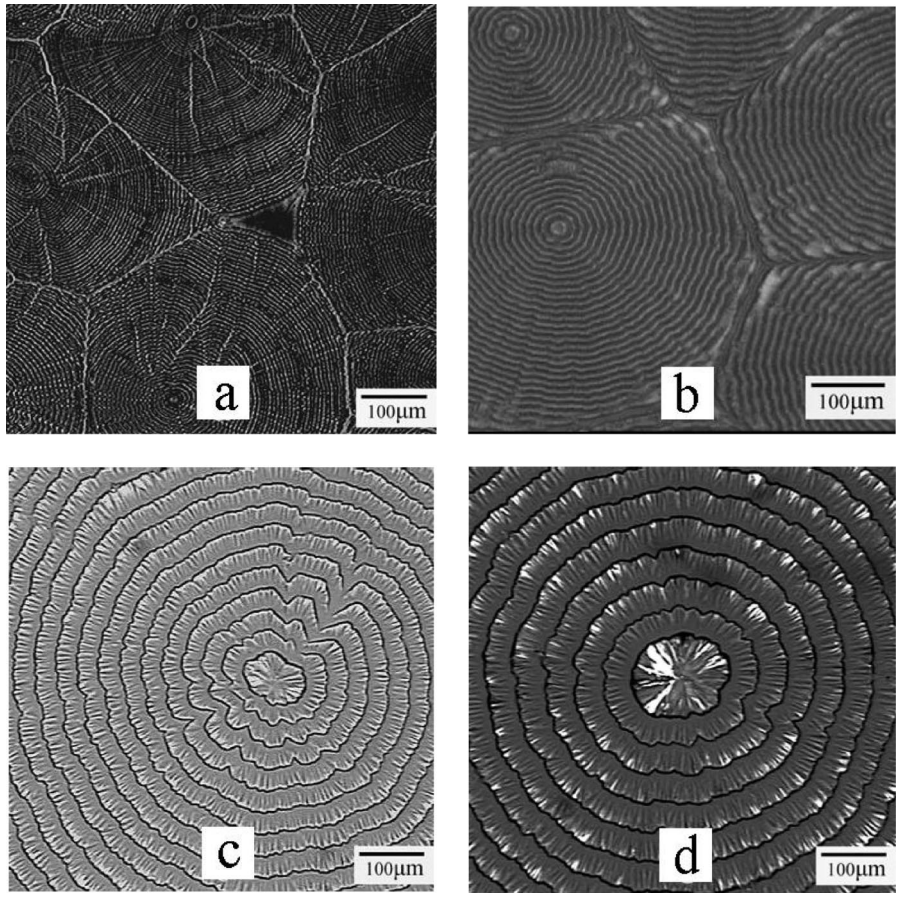

Figure 10. Effect of solution concentration on the morphology of PCL ring-banded spherulites grown at 20 °C during evaporation of solvent at the rate of 1.50×10^{-4} mL/h. Micrographs were taken in cross-polarized light. The concentrations were (a) 5 mg/mL, (b) 10 mg/mL, (c) 20 mg/mL, and (d) 50 mg/mL.

spacing are unavoidable when the constant concentration condition are met at some time during the development of the spherulites because the newly built balance between the growth of spherulites and the evaporation of solvent is not stable enough.

The above results indicate that, for a given molecular weight PCL, the periodic variation of thickness along the radius of ring-banded spherulites is strongly dependent on the initial solution concentration ϕ_i and on the solvent evaporation rate R_{se}. In Table 1, the effect of ϕ_i and R_{se} on the morphological features and the ring spacing is reported. Relatively low ϕ_i and slow R_{se} lead to development of nonbirefringent banded spherulites; an increase of either ϕ_i or R_{se} promotes the formation of birefringent banded spherulites. However, only nonbanded spherulites are generated above a certain concentration and at fast evaporation rate. As shown in the table, the band spacing becomes larger when ϕ_i or R_{se} is increased. A 10 times increase of ϕ_i, from 5 to 50 mg/mL, makes the band spacing to increase roughly the same ratio, from 5.46 to 48.2 μm. On the other hand, a ca. 20 times increase of R_{se}, from 1.50×10^{-4} to 2.80×10^{-3} mL/h, only produces a ca. 8 times increase of the band spacing, from 5.46 to 42.6 μm. From this experimental evidence, it is deduced that the concentration has stronger effect than the evaporation rate on the periodicity of rhythmic growth. In fact, increasing the evaporation rate is an indirect and less effective way of increasing the time-averaged concentration of the solution in close proximity of the growth front.

According to the whole collection of experimental results, it emerges that the formation of ring-banded spherulites with periodic variation of thickness along the growth direction is strongly related to δ, the amount of polymer chains per unit volume which are able to reach the crystallization front from the bulk of the solution. But to which factor the change from nonbirefringent to birefringent ring-banded spherulites has to be attributed? The lamellar crystal's growth velocity should be the key factor governing the formation of the two kinds of ring-banded spherulites. In the development of these spherulites, which are multilayer ensembles of lamellar crystals, the orientation of the lamellae is dictated by the growth velocity of individual layers, rather than by the growth velocity of the whole spherulite. In fact, the growth velocity of each layer is faster than that of the spherulite because new lamellar crystal layers grow upward via screw dislocations. To compare the growth velocity of each layer of lamellar crystal in different spherulites, the growth velocity of spherulites with different thicknesses was normalized to the growth velocity of lamellar crystals with the same thickness V_r referred to the film thickness obtained from 5 mg/mL solution as criterion. According to the above results, nonbirefringent ring-banded spherulites form with the V_r of 4.36 nm/s from 5 mg/mL solution at the R_{se} of 1.03×10^{-3} mL/h (Figure 11b), whereas birefringent ring-banded spherulites form with the V_r of 9.65 nm/s from 5 mg/mL solution at the R_{se} of 2.80×10^{-3} mL/h (Figure 11c). Similar change has been found in solutions with different ϕ_i. Nonbirefringent ring-banded spherulites form with the V_r of 4.00 nm/s from 10 mg/mL solution at the R_{se} of 1.50×10^{-4} mL/h (Figure 10b), whereas birefringent ring-banded spherulites form with the V_r of 10.8 nm/s from 20 mg/mL solution at the R_{se} of 1.50×10^{-4} mL/h (Figure 10c). It is generally believed that nonadjacent re-entry of chains to the crystal and looseness of fold loops introduce overcrowding and inefficient packing in the rapid growth of lamellar crystals, while the different conditions of the formation

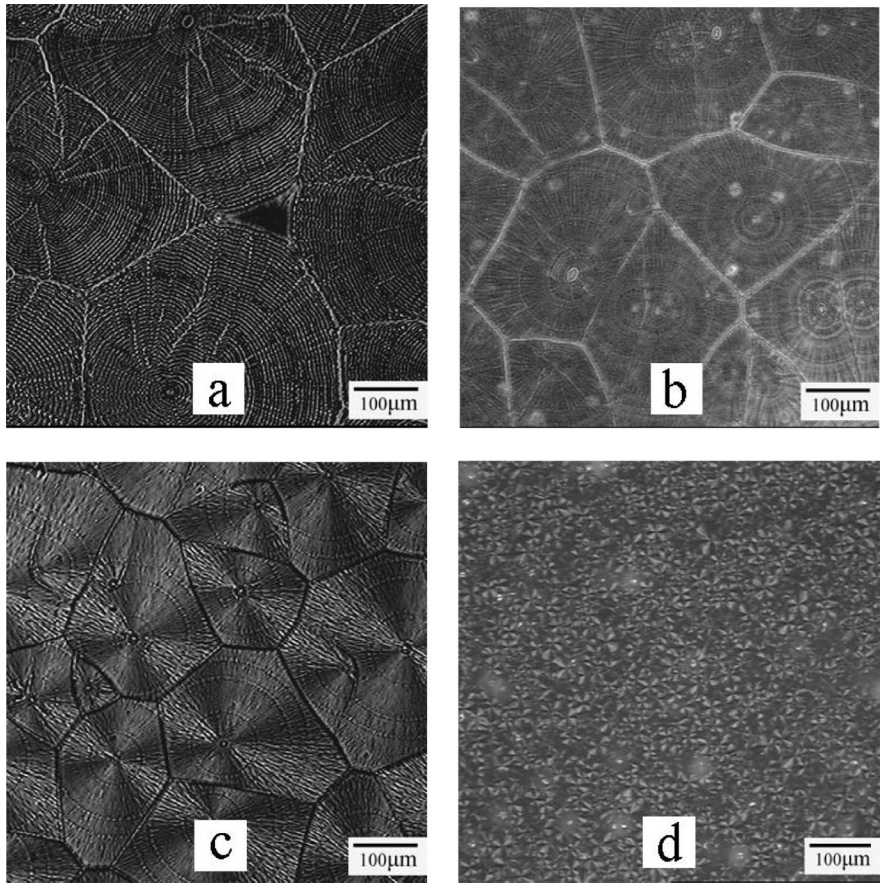

Figure 11. Micrographs in cross-polarized light of PCL spherulites grown at 20 °C from 5 mg/mL toluene solution while the solvent was evaporated at (a) 1.50×10^{-4} mL/h, (b) 1.03×10^{-3} mL/h, (c) 2.80×10^{-3} mL/h, and (d) 6.92×10^{-2} mL/h.

Table 1. Effect of Solution Concentration and Solvent Evaporation Rate on the Formation of PCL Ring-Banded Spherulites at 20 °C

band spacing(μm) / solution concentration (mg/mL) / solvent evaporation rate(mL/h)	5	10	20	50
1.50×10^{-4}	5.46±0.56 nonbire frigent	13.2±2.4 nonbire frigent	26.3±3.8 bire frigent	48.2±4.2 bire frigent
1.03×10^{-3}	28.3±9.7 nonbire frigent	41.4±10.1 bire frigent	53.9±11.5 bire frigent	non banded
2.80×10^{-3}	42.6±9.5 bire frigent	48.5±9.2 bire frigent	non banded	non banded
6.92×10^{-2}	non banded	non banded	non banded	non banded

of opposite fold surfaces lead to a difference in degree of congestion and, hence, in the magnitude of compressive stress. The difference of compressive stress finally results in twisting of lamellar crystals. Furthermore, the faster the growth of the crystal, the greater would be the dissimilarity between resulting fold surfaces.[30] Therefore, nonbirefringent ring-banded spherulites with flat-on lamellar crystals form at low V_r because polymer chains have enough time to find the "ideal" location for their integration in the crystals. Birefringent ring-banded spherulites form at high V_r because flat-on lamellar crystals, owing to the polymer chains having too short time to find their way to appropriate crystal lattice sites, are prone to incline. Just because both nonbirefringent and birefringent ring-banded spherulites have different growth velocities of lamellar crystals between ridges and valleys owing to different thickness, the ring-banded spherulites with radial periodic variation of thickness can be regarded as rhythmic growth-induced ring-banded spherulites.[31]

Conclusion

By controlling the solvent evaporation rate during the spherulitic growth in PCL solution, we attained the constancy of solution concentration when the increase of concentration due to solvent removal is exactly balanced by the depletion of concentration associated to the growth of the crystals. PCL ring-banded spherulites with radial periodic variation of thicknesses were obtained from solution with constant concentration. Nonbirefringent ring-banded spherulites form with slow lamellar crystal's growth velocity at slow solvent evaporation rate from dilute solution, and birefringent ring-banded spherulites form with fast lamellar crystal's growth velocity at fast solvent evaporation rate from concentrated solution. Alternating ridge bands and valley bands of both kinds of ring-banded spherulites are a manifestation of periodic variation of thicknesses along the radius. But in the birefringent ring-banded spherulites, not the same as nonbirefringent ring-banded spherulites, the lamellae rotate out of the film plane as the distance normal to the substrate increases. A periodic diffusion-induced rhythmic growth mechanism associated to periodical change in the concentration gradient was proposed to explain the formation of the ring-banded spherulites with radial periodic variation of thicknesses. The formation process reflects the competition between diffusion flux of polymer chains in solution, J, and spherulitic growth with radial growth velocity, V, which can be characterized by the parameter $\delta = J/V$. Crystallization conditions which have significant influences on δ, including polymer molecular weight, initial solution concentration, and solvent evaporation rate, affect

the formation of PCL ring-banded spherulites with radial periodic variation of thicknesses.

Acknowledgment. The authors thank Prof. Decai Yang at the State Key Laboratory of Polymer Physics and Chemistry of the Changchun Institute of Applied Chemistry for helpful discussions, and Ms. Guifen Sun for technical help for microtomy. This work was supported by the National Science Foundation of China (20574068).

References and Notes

(1) Sakai, Y.; Imai, M.; Kaji, K.; Tsuji, M. *Macromolecules* **1996**, *29*, 8830–8834.
(2) Reiter, G.; Sommer, J. U. *Phys. Rev. Lett.* **1998**, *80*, 3771–3774.
(3) Reiter, G.; Sommer, J. U. *J. Chem. Phys.* **2000**, *112*, 4376–4383.
(4) Sommer, J. U.; Reiter, G. *J. Chem. Phys.* **2000**, *112*, 4384–4393.
(5) Reiter, G.; Castelein, G.; Sommer, J. U. *Phys. Rev. Lett.* **2001**, *86*, 5918–5921.
(6) Wang, M.; Braun, H. G.; Meyer, E. *Macromol. Rapid Commun.* **2002**, *23*, 853–858.
(7) Hu, Z.; Zhang, F.; Huang, H.; Zhang, M.; He, T. *Macromolecules* **2004**, *37*, 3310–3318.
(8) Wang, Z.; Hu, Z.; Chen, Y.; Gong, Y.; Huang, H.; He, T. *Macromolecules* **2007**, *40*, 4381–4385.
(9) Keller, A. *Nature (London)* **1952**, *31*, 913–914.
(10) Keith, H. D.; Padden, F. J. *J. Polym. Sci.* **1959**, *39*, 101–122.
(11) Keller, A. *J. Polym. Sci.* **1959**, *39*, 151–162.
(12) Price, F. P. *J. Polym. Sci.* **1959**, *39*, 139–150.
(13) Ho, R. M.; Ke, K. Z.; Chen, M. *Macromolecules* **2000**, *33*, 7529–7537.
(14) Wang, B. J.; Li, C. Y.; Hanzlicek, J.; Cheng, S. Z. D.; Geil, P. H.; Grebowicz, J.; Ho, R. M. *Polymer* **2001**, *42*, 7171–7180.
(15) Gazzano, M.; Focarete, M. L.; Riekel, C.; Ripamonti, A.; Scandola, M. *Macromol. Chem. Phys.* **2001**, *202*, 1405–1409.
(16) Keith, H. D.; Padden, F. J. *Macromolecules* **1996**, *29*, 7776–7786.
(17) Sasaki, S.; Sakaki, Y.; Takahara, A.; Kajiyama, T. *Polymer* **2002**, *43*, 3441–3446.
(18) Duan, Y. X.; Jiang, Y.; Jiang, S. D.; Li, L.; Yan, S. K.; Schultz, J. M. *Macromolecules* **2004**, *37*, 9283–9286.
(19) Duan, Y. X.; Zhang, Y.; Yan, S. K.; Schultz, J. M. *Polymer* **2005**, *46*, 9015–9021.
(20) Wang, Y.; Chan, C. M.; Li, L.; Ng, K. M. *Langmuir* **2006**, *22*, 7384–7390.
(21) Lauritzen, J. I.; Hoffman, J. D. *J. Res. Natl. Bur. Std.* **1960**, *64A*, 73–102.
(22) Crescenzi, V.; Manzini, G.; Calzolari, G.; Borri, C. *Eur. Polym. J.* **1972**, *8*, 449–463.
(23) Chatani, Y.; Okita, Y.; Tadokoro, H.; Yamashita, Y. *Polym. J.* **1970**, *1*, 555.
(24) Keith, H. D.; Padden, F. J.; Russell, T. P. *Macromolecules* **1989**, *22*, 666–675.
(25) Nunez, E.; Gedde, U. W. *Polymer* **2005**, *46*, 5992–6000.
(26) Iwata, T.; Doi, Y. *Polym. Int.* **2002**, *51*, 852–858.
(27) Henisch, H. K. *Crystals in Gels and Liesegang Rings*; Cambridge University Press: Cambridge, UK, 1988.
(28) Du, Z. X.; Yang, Y.; Xu, J. T.; Fan, Z. Q. *J. Appl. Polym. Sci.* **2007**, *104*, 2986–2991.
(29) Wang, Z.; He, T., unpublished results.
(30) Keith, H. D.; Padden, F. J. *Polymer* **1984**, *25*, 28–42.
(31) Kyu, T.; Chiu, H. W.; Guenther, A. J.; Okabe, Y.; Saito, H.; Inoue, T. *Phys. Rev. Lett.* **1999**, *83*, 2749–2752.

MA8005697